

## PDF hosted at the Radboud Repository of the Radboud University Nijmegen

The following full text is a preprint version which may differ from the publisher's version.

For additional information about this publication click this link.

<http://hdl.handle.net/2066/72410>

Please be advised that this information was generated on 2019-11-17 and may be subject to change.

# Tuning the gap in bilayer graphene using chemical functionalization: DFT calculations

D. W. Boukhvalov\* and M. I. Katsnelson

*Institute for Molecules and Materials, Radboud University of Nijmegen, NL-6525 ED Nijmegen, the Netherlands*

(Dated: July 24, 2008)

Opening, in a controllable way, the energy gap in the electronic spectrum of graphene is necessary for many potential applications, including an efficient carbon-based transistor. We have shown that this can be achieved by chemical functionalization of bilayer graphene. Using various dopants, such as H, F, Cl, Br, OH, CN, CCH, NH<sub>2</sub>, COOH, and CH<sub>3</sub> one can vary the gap smoothly between 0.64 and 3 eV and the state with the energy gap is stable corresponding to the lowest-energy configurations. The peculiarities of the structural properties of bilayer graphene in comparison with bulk graphite are discussed.

PACS numbers: 73.20.Hb, 71.15.Nc, 81.05.Uw, 61.46.Np, 61.48.De, 72.80.-r

## I. INTRODUCTION

Graphene, a recently discovered two-dimensional allotrope of carbon (for review, see Refs.1,2,3) is a very promising material for future development of electronics, due to its planar geometry and a very high electron mobility<sup>1</sup>. Investigations of graphene create a new, unexpected bridge between condensed matter physics and quantum electrodynamics (for review, see Ref.4). At the same time, some of the exotic quantum phenomena which make graphene so attractive scientifically can be considered as obstacles for applications. In particular, the chiral “Klein” tunneling<sup>5</sup> makes  $p - n - p$  (or  $n - p - n$ ) junctions unusually transparent. This does not allow to lock the junction making its use as a transistor problematic. Bilayer graphene<sup>6</sup> is preferable in this sense since the angular range of anomalous transparency is narrower there<sup>5</sup> but only the opening of a real gap in electron spectrum would be a radical solution of the problem. The gapless conical spectrum in the single-layer graphene is very robust; actually, it is protected topologically, assuming that one does not break the sublattice equivalence<sup>7</sup>. The latter can be done, e.g., in a hypothetical bilayer system consisting of a single-layer graphene and a single-layer hexagonal boron nitride<sup>8</sup> but the gap which can be opened in this way is rather small, only about 50 meV. The robustness of the gapless state in the single-layer graphene was demonstrated in recent electronic structure calculations for hydrogenated graphene<sup>9</sup>. It turns out that the gap opens in this case only at 75% coverage. In bilayer graphene, the gap can be opened by applying a strong electric field perpendicular to the graphene plane, as it was demonstrated by recent experimental<sup>10,11</sup> and theoretical<sup>12,13</sup> investigations. In this case the gap is tunable but, again, only in some restricted limits, not larger than the middle infrared region.

Chemical modification of bilayer graphene seems to be a natural way to tune the gap in broader range, from zero to the values typical for conventional semiconductors such as silicon or GaAs. This is the subject of the present work. It is shown that, in contrast with the case of single-layer graphene, the gap opens for dopant concentrations corresponding to the most stable configuration.

## II. COMPUTATIONAL METHOD

We used the SIESTA package for electronic structure calculations<sup>14,15</sup> with the generalized gradient approximation for the density functional<sup>16</sup>, with the energy mesh cutoff of 400 Ry, and a  $k$ -point  $11 \times 11 \times 1$  mesh in the Monkhorst-Park scheme<sup>17</sup>. This method is frequently used for computations of the electronic structure of single-layer graphene<sup>9,18,19,20</sup>.

It is known<sup>21,22,23</sup> that the use of GGA leads to essential overestimate of the equilibrium interlayer distances for layered compounds, such as graphite, hexagonal boron nitride (hBN), and MoS<sub>2</sub>, due to the inadequate description of the van der Waals interaction effects. On the other hand, the LDA slightly underestimates these distances<sup>21,24</sup>. However, all these calculations have been carried out for three-dimensional crystals where each layer interacts with *two* neighboring layers and it is not clear *a priori* what is the situation for a bilayer. Structural properties of bilayer graphene are different from both bulk graphite and single-layer graphene, as is confirmed by measurements of the Raman spectra<sup>25</sup> and characteristics of ripples on the bilayer<sup>26</sup>. Peculiarities of structural states of bilayers in comparison with bulk crystals were observed also in ionic crystals such as wurtzite ZnO(0001)<sup>27</sup>.

To check the applicability of different approximations we have carried out LDA and GGA calculations of structural properties of the multilayers of graphene and hBN. The LDA computational results are shown in Fig. 1. One can see that the total energy per atom almost coincides with that for bulk graphite starting with approximately five layers (with the accuracy of 1 meV), in qualitative agreement with the conclusions from Raman spectra<sup>25</sup>. The energy difference between bilayer and single-layer is approximately the same as between the bulk crystal and bilayer, both for carbon and for BN.

Interestingly, the equilibrium interlayer distances for bilayer graphene and hBN differ only within 10% (Fig. 2) which is much smaller than for the bulk<sup>21</sup>. Our SIESTA computational results for the latter case coincides within 1% with those of FLAPW calculations<sup>21</sup> so this difference is rather due to the difference of the systems themselves

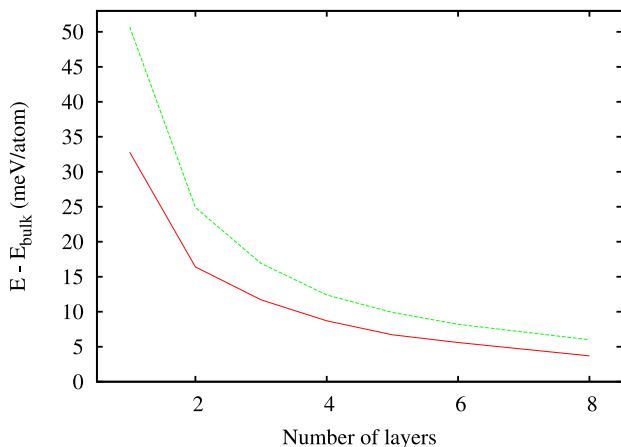


FIG. 1: (color online) Total energies per atom for multilayer graphene (solid red line) and hexagonal BN (dashed green line) counted from those for bulk, as functions of number of layers.

than of the methods used. It is worthwhile to note that the curves of energy versus interlayer distance are essentially different for the bulk and for the bilayer.

Thus, LDA and GGA computational results are much closer for the case of bilayers than for the case of bulk layered crystals. In the following, we will discuss in more detail only the GGA data since GGA gives better results for chemisorption energies and bond lengths<sup>9</sup>. Anyway, neither LDA nor GGA allows to calculate accurately energy gaps<sup>28</sup> and the corresponding results are rather estimations from below. At the same time, as we will see, that the energy gap grows as the interlayer distance decrease so the GGA overestimating interlayer distances gives surely the lower estimation whereas, in the case of LDA, the error can be, in principle, of any sign.

Recent electronic structure calculations for hydrogenized graphene<sup>9</sup> demonstrate that it is more favorable energetically to attach dopants to carbon atoms belonging to different sublattices, which allows to avoid the formation of dangling bonds. Minimization of geometric frustration of the carbon lattice is another important factor determining the stable configurations. Fig. 3a displays schematically the distortion of single-layer graphene for chemisorption of single hydrogen atom: the carbon atom connected with hydrogen is shifted up whereas its nearest and next-nearest neighbors are displaced down and the third neighbors are shifted up again. The most stable configuration for the case of single-layer graphene correspond to bonding of hydrogen with neighboring carbon atoms at opposite sides (positions 1 and 2, according to the standard chemical terminology). If one allows only the one-side chemisorption than (1,4) positions of hydrogens turn out to be optimal, that is, bonding with third neighbors (Fig. 3b). In that case distortions of positions of other carbon atoms will be similar to those for (1,2) bonding (nearest and next nearest neighbors are shifted down). For the bilayer only one side of each graphene

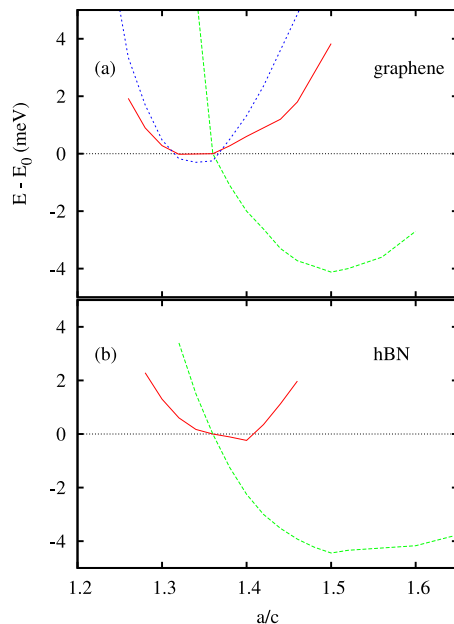


FIG. 2: (color online) Total energies per atom as functions of the ratio of interlayer distance  $c$  to in-plane lattice constant  $a$  for graphene (a) and hexagonal BN (b); solid red and dashed green lines correspond to LDA and GGA, respectively, dotted blue line corresponds to the LDA calculations for bulk graphite. Here  $E_0$  is the energy of bilayer with lattice parameters corresponding to the bulk.

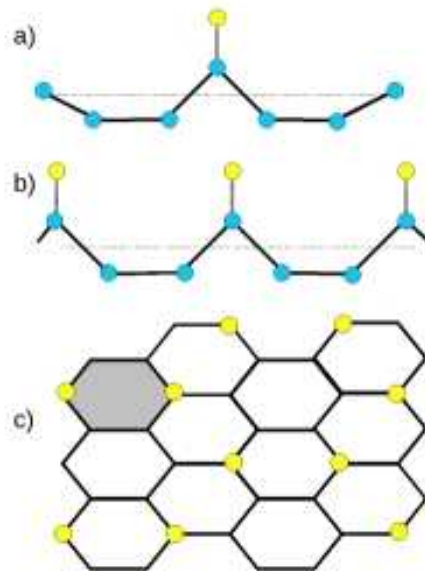


FIG. 3: (color online) A sketch of atomic positions for hydrogenated graphene: (a) A single hydrogen atom; (b) the most stable configuration for the chemisorption at one side; (c) the maximum coverage for the chemisorption at one side (a top view). Blue circles are carbon atoms, yellow ones are hydrogens, the grey hexagon corresponds to the atomic group shown in Figs. 4 and 6.

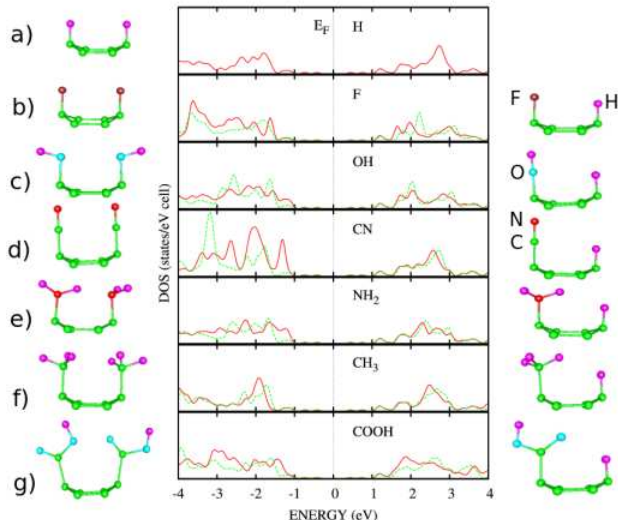


FIG. 4: (color online) Optimized configurations and total densities of states for one-side functionalization of bilayer graphene. Left panel and red solid lines correspond to the case of two identical dopants, e.g., F...F, per hexagon; right panel and dashed green lines correspond to the case when one dopant group per hexagon is replaced by hydrogen atom, e.g. F...H.

layer is available so one can expect an optimal configuration similar to shown in Fig. 3b. One can expect that these arguments are applicable not only to hydrogen but to other dopants, and this is confirmed, indeed, by our computational results.

This leads to the important consequence that the maximum coverage for the bilayer should be about 25%, otherwise first and second neighbors are filled unavoidably. Contrary, for the case of single-layer graphene where both sides are available the configuration with one hydrogen atom per carbon atom is the most energetically favorable<sup>9</sup>. The optimal one-side coverage of bilayer is sketched in Fig. 3c.

### III. RESULTS AND DISCUSSIONS

First, we have investigated the dependence of the total energy on the type of dopant and its concentration (coverage level). We have found that the most stable configurations occurs for functionalization by fluorine and hydroxyl groups (the case of hydrogen was considered in Ref.<sup>9</sup>). The supercell size was varied between 32 to 8 carbon atoms per layer (the latter corresponds to a maximum possible 25% coverage, two dopant atoms or molecules per eight carbon atoms). The chemisorption energy was calculated as described in Ref.9, choosing molecular fluorine  $F_2$  and water  $H_2O$  as reference points for the cases of F and OH, respectively. The calculations show a decrease of the chemisorption energy with coverage (in the limits noticed above), from - 1.58 eV to -

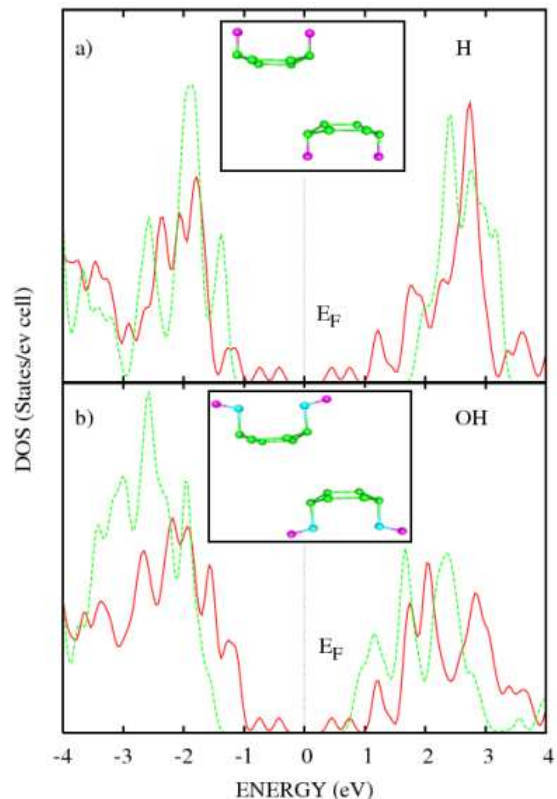


FIG. 5: (color online) Total densities of states for one-side (solid red lines) and two-side (dashed green lines) functionalization of bilayer graphene, for the case of hydrogen (a) and hydroxyl (b). Insets show optimized atomic configurations for the case of two-side functionalization.

1.89 eV for F and from -2.37 eV to -3.16 eV for OH. In both cases, as well as for H, the most stable configurations correspond to the maximum coverage. While for single H atom the activation energy is positive (1.28 eV) and thus its chemisorption is not favorable, for F and OH the corresponding values are -1.21 eV and -2.23 eV, respectively.

Further, we have considered also the one-side functionalization of bilayer graphene by other groups, namely, CN,  $NH_2$ ,  $CH_3$ , COOH, as well as by combination of the dopants and hydrogen (see Fig. 4). Despite a rather different chemical composition of dopants the distortions of the functionalized graphene layer the height differences between the highest and the lowest positions of carbon atoms in the layer  $d$  lie in a relatively narrow interval, from 0.36 Å for the case of H to 0.57 Å for the case of COOH (see Fig. 4g), that is, from 11% to 17% of interlayer distance in graphite (3.35 Å). The minimal interlayer distances  $h$  in the one-side functionalized bilayer vary between 3.25 Å for H and 2.98 Å for COOH (97%-89% of interlayer distance in graphite).

The electronic structure for the most stable configuration (25% coverage) is shown in Figs. 4 and 5. One can see that, surprisingly, the value of the energy gap opening

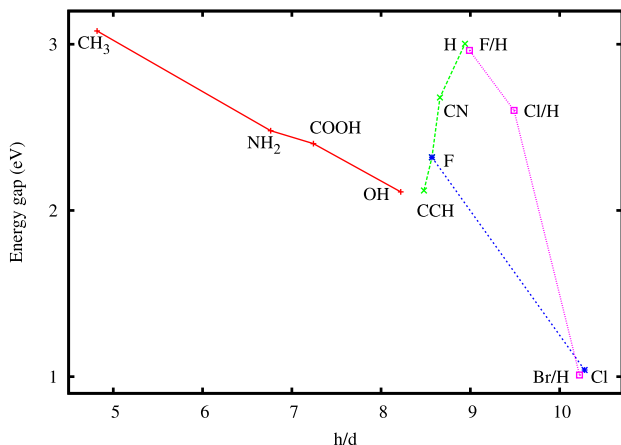


FIG. 6: (color online) Energy gap values for the case of two-side functionalization of bilayer graphene, as a function of the ratio of the interlayer distance  $h$  to the carbon atom distortion  $d$ .

as a function of doping is not too sensitive to the dopant type varying in the interval 0.64 - 0.68 eV (see Fig. 6). In a sense, the situation reminds the epitaxial graphene on SiC<sup>29</sup> where one graphene layer is supposed to be almost unperturbed and another one (buffer layer) is strongly coupled covalently with the substrate. For some types of epitaxial graphene, the existence of energy gap was theoretically predicted (0.45 eV, Ref.30) and experimentally confirmed (0.26 eV, Ref.31). Interestingly, some peaks of the density of states around the Fermi energy have been observed there<sup>31</sup>. Similar peaks can be seen also in our computational results (Fig. 4 and 5).

Further, we have investigated the case of two-side functionalization. It was shown already that for the case of hydrogen, one-side and two-side chemisorption energies of bilayer graphene are rather close<sup>9</sup>. The same turns out to be the case also for the case of fluorine and hydroxyl group. At the same time, the electronic structures for the case of one-side and two-side doping are completely different. For the latter case, the energy gap is essentially larger varying from 2.12 eV for hydroxyl group to 3.03 eV for hydrogen (see Fig. 5). In the case of one-side functionalization a hybridization with practically unperturbed layer of pure graphene holds whereas for the two-side case both layers are strongly modified and distorted.

We now discuss the equilibrium configurations of the dopants shown in Figs. 4 and 5. For single atoms such as H and F it is impossible to discuss their orientation, and for the case of CN group a very strong triple C-N bond keeps the molecule normal to the graphene plane. For other cases, the dopant orientations are coordinated by their interactions. This is clearly seen, e.g., for OH group in Fig. 4 and inset to Fig. 5b. While for a single OH group the angle C-O-H is almost 180° for neighboring OH groups, this angle diminishes to 105° and a preferable mutual orientation of the groups appear, for both one-side and two-side doping (see inset

to Fig. 3b for the latter case). For the dopants of this type, actually, a four-layer system is formed, such as dopant/carbon/carbon/dopant. This leads to specific dopant-dependent distortions of graphene affecting the value of the energy gap. The stronger distortion and, therefore, the weaker the interaction between the dopants at opposite sides of graphene, the larger is the energy gap. For the different single-atom dopants under consideration, the distortions are more or less the same and the gap is mainly dependent on their number in the Periodic Table. These data are summarized in Fig. 4.

We have performed also calculations for CCH dopant, with the triple C-C bond. In this case, as well as for CN, the dopant orientation is irrelevant, and the value of the gap continues the line H-CN-F... (Fig. 6).

We have considered also different combinations of the dopants with hydrogen. The latter destroys the ordered four-layer structure described above and the values of energy gap turn out to be close for all the dopants varying in the limits 2.96 - 3.03 eV.

Next, we have investigated the effect of surrounding water for the case of hydroxyl groups. If one adds one water molecule per group connected by the hydrogen bond and optimize the structure it leads to additional distortions of the bilayer (0.39 Å without water and 0.51 Å with water) increasing the value of energy gap from 2.12 to 2.36 eV.

We have considered also the doping of bilayer by heavier elements, namely, halogens Cl and Br. However, in these cases the limitations because of size factors become more essential. Whereas doping of the bilayer by chlorine is possible two bromine atoms form stable molecule B<sub>2</sub> under the surface of practically undistorted bilayer. However, partial doping by heavy halogens is possible if combine them with hydrogen. The values of energy gap for F...H and Cl...H doping are larger than for F...F and Cl...Cl, respectively (see Fig. 6).

#### IV. CONCLUSION

To conclude, our results allow to formulate general principles determining the value of energy gaps in doped bilayer graphene. One-side doping, almost independently on the chemical nature of the dopants, leads to gaps of the order of 0.6 - 0.7 eV. Two-side doping makes possible to change the gap in much broader limits. The functionalization by halogens or their combination with hydrogen results in gap values in the range 1 to 3 eV, however, this value cannot be fine tuned. On the other hand, using various groups formed by elements of the second period of the Periodic table one can change the gap between 2 and 3 eV smoothly, with the accuracy about 0.2 eV. Interaction between dopants and water can also change the gap by a value of order of 0.2 eV. Thus, variations of solvents can be also used to tune the gap. The case of hydroxyl groups requires further more detailed investigation due to its relevance for perspective exfoliated graphene oxide<sup>32</sup>.

## V. ACKNOWLEDGEMENTS

Netherlands.

The work is financially supported by Stichting voor Fundamenteel Onderzoek der Materie (FOM), the

- 
- \* Electronic address: D.Bukhvalov@science.ru.nl
- <sup>1</sup> A. K. Geim, and K. S. Novoselov, *Nature Mater.* **6**, 183 (2007).
  - <sup>2</sup> M. I. Katsnelson, *Mater. Today* **10**, 20 (2007).
  - <sup>3</sup> A. H. Castro Neto, F. Guinea, N. M. R. Peres, K. S. Novoselov, A. K. Geim, arXiv:0709.1163 (to appear in *Rev. Mod. Phys.*).
  - <sup>4</sup> M. I. Katsnelson, and K. S. Novoselov, *Solid State Commun.* **143**, 3 (2007).
  - <sup>5</sup> M. I. Katsnelson, K. S. Novoselov, A. K. Geim, *Nature Phys.* **2**, 620 (2006).
  - <sup>6</sup> K. S. Novoselov, E. McCann, S. V. Morozov, V. I. Fal'ko, M. I. Katsnelson, U. Zeitler, D. Jiang, F. Schedin, A. K. Geim, *Nature Phys.* **2**, 177 (2006).
  - <sup>7</sup> J. L. Mañes, F. Guinea, M. A. H. Vozmediano, *Phys. Rev. B* **75**, 155424 (2007).
  - <sup>8</sup> G. Giovannetti, P. A. Khomyakov, G. Brocks, P. J. Kelly, J. van den Brink, *Phys. Rev. B* **76**, 073103 (2007).
  - <sup>9</sup> D. W. Boukhvalov, M. I. Katsnelson, A. I. Lichtenstein, *Phys. Rev. B* **77**, 035427 (2008).
  - <sup>10</sup> E. V. Castro, K. S. Novoselov, S. V. Morozov, N. M. R. Peres, J. M. B. Lopes dos Santos, J. Nilsson, F. Guinea, A. K. Geim, A. H. Castro Neto, *Phys. Rev. Lett.* **99**, 216802 (2007).
  - <sup>11</sup> J. B. Oostinga, H. B. Heersche, X. Liu, A. F. Morpurgo, L. M. K. Vandersypen, *Nature Mater.* **7**, 151 (2008).
  - <sup>12</sup> E. McCann, *Phys. Rev. B* **74**, 161403(R) (2006).
  - <sup>13</sup> H. Min, B. Sahu, S. K. Banerjee, A. H. MacDonald, *Phys. Rev. B* **75**, 155115 (2007).
  - <sup>14</sup> E. Artacho, J.D. Gale, A. Garsia, J. Junquera, R.M. Martin, P. Orejon, D. Sanchez-Portal, J.M. Soler, SIESTA, Version 1.3, 2004.
  - <sup>15</sup> J.M. Soler, E. Artacho, J.D. Gale, A. Garsia, J. Junquera, P. Orejon, D. Sanchez-Portal, *J. Phys.: Condens. Matter* **14**, 2745 (2002).
  - <sup>16</sup> J.P. Perdew, K. Burke, and M. Ernzerhof, *Phys. Rev. Lett.* **77**, 3865 (1996).
  - <sup>17</sup> H. J. Monkhorst, and J. D. Park, *Phys. Rev. B* **13**, 5188 (1976).
  - <sup>18</sup> O. V. Yazyev, and L. Helm, *Phys. Rev. B* **75**, 125408 (2007).
  - <sup>19</sup> Y.-W. Son, M. L. Cohen, S. G. Loui, *Nature (London)* **444**, 347 (2006).
  - <sup>20</sup> W. L. Wang, S. Meng, and E. Kaxiras, *Nano Lett.* **8**, 241 (2008).
  - <sup>21</sup> A. Janotti, S.-H. Wei, and D. J. Singh, *Phys. Rev. B* **64**, 174107 (2001).
  - <sup>22</sup> H. Rydberg, M. Dion, N. Jacobson, E. Schroder, P. Hyldgaard, S. I. Simak, D. C. Langreth, and B. I. Lundqvist, *Phys. Rev. Lett.* **91**, 126402 (2003).
  - <sup>23</sup> A. Marini, P. García-González, and A. Rubio, *Phys. Rev. Lett.* **96**, 136404 (2006).
  - <sup>24</sup> M. C. Schabel, and J. L. Martins, *Phys. Rev. B* **46**, 7185 (1992).
  - <sup>25</sup> A. C. Ferrari, J. C. Meyer, V. Scardaci, C. Casiraghi, M. Lazzeri, F. Mauri, S. Piscanec, D. Jiang, K. S. Novoselov, S. Roth, and A.K. Geim, *Phys. Rev. Lett.* **97**, 187401 (2006).
  - <sup>26</sup> J. C. Meyer, A. K. Geim, M. I. Katsnelson, K. S. Novoselov, D. Obergfell, S. Roth, C. Girit, and A. Zettl, *Solid State Commun.* **143**, 101 (2007).
  - <sup>27</sup> C. Tusche, H. L. Meyerheim, and J. Kirschner, *Phys. Rev. Lett.* **99**, 026102 (2007).
  - <sup>28</sup> L. Yang, C.-H. Park, Y.-W. Son, M. L. Cohen, and S. G. Louie, *Phys. Rev. Lett.* **99**, 186801 (2007).
  - <sup>29</sup> C. Berger, et al. *Science* **312**, 1191 (2006).
  - <sup>30</sup> A. Mattausch, O. Pankratov, *Phys. Rev. Lett.* **99**, 076802 (2007).
  - <sup>31</sup> S. Y. Zhou, G.-H. Gweon, A. V. Fedorov, P. N. First, W. A. de Heer, D.-H. Lee, F. Guinea, A. H. Castro Neto, A. Lanzara, *Nature mater.* **6**, 770 (2007).
  - <sup>32</sup> S. Stankovich, D. A. Dikin, G. H. B. Dommett, K. M. Kohlhaas, E. J. Zimney, E. A. Stach, R. D. Piner, S. T. Nguyen, R. S. Ruoff, *Nature (London)* **442**, 282 (2006).